Drug Development and Industrial Pharmacy, 2011; 37(12): 1402–1414

ISSN 0363-9045 print/ISSN 1520-5762 online
DOI: 10.3109/03639045.2011.580350

informa
healthcare

RESEARCH ARTICLE

Mupirocin calcium microencapsulation via spray drying: feed solvent influence on microparticle properties, stability and antimicrobial activity

Marjana Dürrigl[1], Maja Lusina Kregar[1], Anita Hafner[2], Maja Šegvić Klarić[2], and Jelena Filipović-Grčić[2]

[1]Pliva Croatia Ltd, Research and Development, Zagreb, Croatia, and [2]University of Zagreb, Faculty of Pharmacy and Biochemistry, Zagreb, Croatia

Abstract

Objectives: The aim of this research was to design a controlled release, spray dried, mupirocin calcium-loaded microparticles (MP) with acrylic polymer and assess the influence of a feed solvent at preselected drug:polymer proportions (1:5 and 2:1 (w/w)) on the performance and stability of the prepared MP.

Methods: Physicochemical properties of MP were assessed using modulated differential scanning calorimetry (MDSC), and thermogravimetric analyses (TGA), Fourier transformed infrared spectroscopy (FTIR) and X-ray analyses and were correlated with drug release. Morphology and particle size were determined using low-angle laser light scattering and a scanning electron microscope. A time-kill assay was conducted on two strains of *Staphylococcus aureus* to evaluate the antimicrobial activity of MP.

Results and discussion: The MP formed solid dispersions without apparent drug crystallization. Drug-polymer miscibility, morphology, drug release and consequently antimicrobial activity were dependent on drug loading (DL) and the used solvent. The superior control of drug release from MP was achieved for the higher DL (2:1 (w/w) drug:polymer proportion) using solvents in the following order: methanol ≈ methanol:ethanol (50:50, w/w) > isopropanol:acetone (40:60, w/w). Moreover, a time-kill assay performed on *S. aureus* (ATCC 29213) and methicillin-resistant *S. aureus* strains confirmed the prolonged release and preservation of antimicrobial activity of the microencapsulated drug. The physical aging of the solid dispersion after 10 months of storage had negligible impact on the MP performance.

Conclusions: Acrylic-based MP were confirmed as suitable microcarriers for prolonged drug release using a well-established spray drying technique, while solvent influence was strongly related to the DL employed.

Keywords: Mupirocin calcium, spray drying, solid dispersions, controlled release, microparticles, antimicrobial activity, stability

Introduction

The spray drying technique has been used as a microencapsulation method, being able to create microparticles (MP) composed of drug and polymer that were previously dissolved, dispersed or emulsified in the appropriate aqueous or organic medium[1]. Pharmaceutical MP preparation using the spray drying process includes not only the removal of solvent and reduction of particle size, but also the generation of the particles that have a well-defined morphology and physicochemical properties[2]. The encapsulation of a drug within a polymer allows for greater control of the pharmacokinetic behavior of the active molecule, maintaining a more appropriate level of the drug at the site of delivery[3], especially where micron size is an advantageous feature (e.g., topical and ocular administration[4,5]).

It is well known that the feed composition and spray drying process determine the ultimate product

Address for Correspondence: Prof. Jelena Filipović-Grčić PhD, Department of Pharmaceutics, Faculty of Pharmacy and Biochemistry, University of Zagreb, A. Kovačića 1, 10000 Zagreb, Croatia. Tel.: +38516394761. Fax: +38514612691. E-mail: jfilipov@pharma.hr.

(Received 13 February 2011; revised 01 April 2011; accepted 05 April 2011)

characteristics[6,7]. Specifically, the solvent used for the feed preparation influences several very important factors that greatly contribute to the final MP properties and performance. It affects the following: (i) polymer solubility as well as the conformation of its chains[8]; (ii) deposition kinetics under constant spray drying conditions that are related to the solvent evaporation rate (determined by the boiling point temperature and heat of vaporization[9,10]) and the initial saturation of constituents. The solvent has a tremendous impact on the MP morphology[10–13] and density, which are directly allied with drug release[14]. Polymer chains have different conformations depending on the ability of the solvent to solubilize the polymer[13,14]. The physical entanglements between polymer chains change in different solvents. In a good solvent, the polymer exhibits a random coil-expanded conformation, whereas in poor solvent and in dilute solution, the polymer chain collapses, producing a globular conformation. Moreover, in poor solvents, polymer-rich and polymer-depleted phases may occur[15], influencing the possibility that the polymer will interact with the other constituents[16]. The solvent evaporation rate and deposition kinetics dictate the matrix coherence and the amount of strain stored in the system. Denser matrices restrict polymer chain mobility due to reduced free volume, simultaneously limiting medium penetration into the MP matrix[14].

Spray drying frequently ends up in a final product of amorphous nature, which is prone to undergo structural relaxation during storage, characterized by enthalpy and volume reduction. Drug release from the MP could change upon storage due to the time and temperature dependant variation of the free volume[17]. The magnitude of the driving force that leads to structural relaxation is linked to the rate of particle formation and is affected by process parameters[18]. Literature reports for poly(lactic-co-glycolic)acid MP indicate that the manufacturing process, residual solvent level and the nature of the interaction between the drug and polymer affect the rate of structural relaxation[18]. Therefore, the conditions directly influencing particle formation (e.g., solvent, initial drug saturation) could be a source of variability in the burst release and may affect the stability of the drug release during storage[17,18].

Esposito et al[11]. earlier evaluated the solvent influence on the morphological and dimensional properties of Eudragit® RS-based MP prepared by spray drying while Sipos et al[19]. examined its impact on thermal properties; however, no data on drug release were provided. Stability of such microsystems, in terms of evaluating changes caused by relaxation processes and other solid-state alterations, has not been previously examined. Therefore, we aimed to broaden the current understanding of solvent influence on the MP physicochemical properties, stability and performance.

This study is a continuation of our previous work on the spray dried Eudragit® RS-based MP with mupirocin calcium[20]. Mupirocin calcium, a topical antibiotic, exerts antimicrobial activity by reversibly inhibiting isoleucyl-transfer RNA, thereby inhibiting bacterial protein and RNA synthesis[21]. It has excellent activity against susceptible strains of *Staphylococcus aureus* and *Streptococcus pyogenes* in the treatment of secondarily-infected traumatic skin lesions as well as against methicillin-resistant *S. aureus* (MRSA) as an intranasal agent. Given that mupirocin was administered three-times daily, with the increased likelihood that this regular dosing regime would be omitted resulting in a reduced curing rate, prolonged release MP were considered in order to improve the therapy. Such MP could provide a prolonged release of the drug on the skin, thus administering the drug in a localized manner at the application site, while simultaneously reducing application frequency[22].

The spray dried powders prepared from two different drug:polymer proportions (1:5 and 2:1 (w/w)) were evaluated in terms of drug loading (DL), yield, encapsulation efficacy, particle size, morphology and drug release. In addition, mathematical modeling was applied to separate burst and sustained phases of the drug release profiles. Solid-state properties were assessed using a number of appropriate and complementary analytical techniques such as powder X-ray diffraction (XRPD), thermogravimetric analyses (TGA), modulated differential scanning calorimetry (MDSC) and Fourier transformed infrared spectroscopy (FTIR). In addition, a time-kill assay was performed using *S. aureus* (ATCC 29213) and clinically isolated methicillin-resistant *S. aureus* (MRSA) strains at two concentrations in order to evaluate the antimicrobial activity of microsystems.

Materials and methods

Materials

Mupirocin calcium was kindly donated by Pliva Croatia Ltd., Zagreb, Croatia. Eudragit® RS 100 and Eudragit® RS 12.5 (12.5% (w/w) of polymer in a 40:60 (w/w) acetone:isopropanol mixture) were obtained from Evonik, Essen, Germany. Methanol and tetrahydrofuran (liquid chromatography grade), ammonium acetate (puriss p.a.) and potassium bromide (grade for infrared spectroscopy) were obtained from Merck KgaA, Darmstadt, Germany. Sodium acetate trihydrate (puriss p.a.) was provided by Kemika, Zagreb, Croatia. Polysorbate 80 was procured from Uniquema, Merseyside, UK. Ultra pure water was used in all the experiments.

Methods

Preparation of MP

MP were prepared by spray drying the solutions containing two different proportions of mupirocin calcium and Eudragit® RS polymer, namely 2:1 and 1:5 (w/w). These proportions were preselected based on preliminary work that was previously published[20]. Samples M and ME were prepared by dissolving Eudragit® RS 100 in methanol and methanol:ethanol (50:50, w/w) respectively, using an

ultrasonic bath until complete dissolution of the polymer was achieved. The polymer solution was then left for 24 h before the drug was added. Mupirocin calcium was easily dissolved in the polymer solution by gentle stirring and spray dried immediately. Samples AI were prepared using commercially available Eudragit® RS 12.5 solution in which acetone:isopropanol (40:60, w/w) was used as the solvent. The total amount of solid material in all feed solutions was 3.0% (w/w).

Spray drying was performed using a Büchi B-290 mini spray dryer (Büchi Labortechnik AG, Flawil, Switzerland) with the Inert Loop B-295, which enabled safe operation with organic solvents in a closed loop. Compressed nitrogen was used to disperse the liquid into fine droplets, which were consequently dried in the cylinder and deposed in the cyclone. Drying conditions are given as follows for all prepared samples: the temperature was 110°C, the aspirator setting was 85%, the pump flow rate was 40% and the compressed nitrogen flow rate was 670 Nl/h. A small high-performance cyclone was used to increase the yield.

Determination of the DL and encapsulation efficiency

The mupirocin calcium content in the MP was determined by the HPLC assay method described in the United States Pharmacopeia (USP), 31st edition, Suppl. 2, 2009. An appropriate amount of MP was dissolved in methanol by sonication in an ultrasonic bath (Julabo USR3, Julabo Labortechnik Gmbh, Seelbach, Germany) for 30 min to obtain 0.1 mg/mL of mupirocin calcium. Samples were filtered through glass fiber prefilters (Acrodisc® GF 25 mm syringe filters with GF/0.45 GHP membrane, Pall, Bad Kreuznach, Germany) before drug determination. An HPLC system, which consisted of an Agilent 1100 Series instrument (Agilent Technologies, Waldbronn, Germany) equipped with a diode array detector set at 230 nm, was used to perform the assay. The mobile phase, a degassed and filtered mixture of 0.1 M ammonium acetate and tetrahydrofuran in the ratio of 68:32, was used at a flow rate of 1 mL/min. The column (Zorbax Eclipse XDB C8 column 250 × 4.6 mm, particle size 5 µm, Agilent, Palo Alto, CA) suited with a guard column (Symmetry C8, particle size 5 µm, 3.9 × 20 mm, Waters, Dublin, Ireland) was operated at 35°C. The sample injection volume was 20 µL. The elution was isocratic and the run time was 10 min. All experiments were performed in triplicate.

DL was determined as a percent ratio (w/w %) of the drug present in the MP. Encapsulation efficiency (EE) was determined as a percent ratio (w/w %) of the actual drug content in MP and the amount of drug added (theoretical content). The yield was calculated by dividing the weight of MP by the total weight of the added ingredients (polymer and drug).

Drug release study

The dissolution test was performed using a USP 31 Apparatus 2 paddle apparatus (PharmaTest type PTW S, PharmaTest Apparatebau GmbH, Hainburg, Germany). A predetermined amount of MP containing 50 mg of the drug was placed into 500 mL of degassed pH 5.5 USP acetate buffer, and the temperature was maintained at 37 ± 0.5°C. The paddle speed was 20 rpm. Aliquots (5 mL) were withdrawn at predetermined time points and analyzed, according to the HPLC assay method described above. The withdrawn aliquots were replaced with fresh dissolution medium thermostated at 37°C. The sink condition of the drug was maintained in a given pH medium. All analyses were performed in triplicate.

Particle size analysis

Measurements of particle size distributions (PSDs) of MP were obtained using a low-angle laser light scattering instrument, Mastersizer 2000 (Malvern Instruments Ltd., Malvern, Worcestershire, UK). Particles were dispersed using a Hydro 2000µP dispersion unit. MP were dispersed in tap water using several drops of 1% (w/w) polysorbate 80 solution as a dispersant. Obscuration was set between 8 and 15%, and the samples were pretreated with internal ultrasound for 1 min at the 100% level. During measurement, the pump/stirrer was set at 2000 rpm, and ultrasound was applied continuously at 10%. The sizes that were quoted are average values of six measurements.

Thermal analyses

MDSC analyses were carried out on a TA Instrument Q1000 Modulated DSC (TA Instruments, New Castle, DE) using aluminum hermetic pans with pierced lids (to allow for removal of residual solvent) with about 5 ± 2 mg of sample, under a dynamic nitrogen atmosphere (50 mL/min). The samples were heated at 5°C/min from 20 to 200°C, using modulation temperature amplitude of ±0.8°C and period of 60 s. The glass transition temperature (T_g) was determined using the TA Universal Analyses 2000 software by extrapolating the linear portion of the DSC curve above and below the glass transition point and determining the midpoint temperature in the reverse heat flow curve. The analyses were performed in triplicate.

Thermogravimetric (TG) curves were obtained using a TGA-7 TG analyzer (Perkin-Elmer Co., Norwalk, CT), using platinum pans with about 5 mg of sample, under a dynamic nitrogen atmosphere (35 mL/min) and at a heating rate of 10°C/min from 30 to 250°C. These analyses enabled the determination of the total amount of volatile substance (residual solvent). The analyses were done in triplicate.

Infrared analyses

Infrared spectra were recorded on a Nicolet 6700 FTIR instrument (Thermo Fisher Scientific Inc., Waltham, MA) equipped with a fast recovery deuterated triglycine sulfate (DTGS) detector, working under Omnic software version 4.1. A spectral range of 400–4000 cm^{-1}, resolution of 4 cm^{-1} and an accumulation of 32 scans were used in order to obtain good-quality spectra. A KBr disc

method was used with approximately 0.5% (w/w) sample loading.

Scanning electron microscopy

The morphology of the MP was observed on a JEOL JSM-5800 scanning electron microscope (SEM) (JEOL, Tokyo, Japan). Samples were mounted on the double-sided adhesive and coated with a thin layer of gold under vacuum. The SEM was operated at an acceleration voltage of 15 kV.

X-ray analyses

XRPD data were recorded on a Philips X'Pert PRO diffractometer (PAN Analytical, Kassel, Waldau, Germany) equipped with an X'Celerator detector (2.022° 2θ) using CuKα radiation at 45 kV and 40 mV. The scan angle range (2θ) was 2–50°, the step size (2θ) was 0.017° and the time per step was 50 s. Samples were powdered in a mortar and applied directly onto a Phillips' original circular sample holder (16 mm diameter) and closed with the bottom plate. Diffractograms were analyzed using X'Pert Data Collector software.

Stability studies

MP stability was assessed after storage for 10 months at controlled room temperature (25°C/60%RH) in glass containers. X-ray, MDSC and drug release analyses were conducted to evaluate the physical stability of the powders.

Antimicrobial activity

The antimicrobial activity of MP was investigated with respect to the free drug. Samples were suspended in degassed acetate buffer (pH 5.5; USP) immediately prior to examination. Antimicrobial activity was tested on *S. aureus* (ATCC 29213) and three clinical isolates of methicillin-resistant *S. aureus* (MRSA). A two-fold microdilution assay using Mueller-Hinton broth (Sigma, Munich, Germany) was carried out following CLSI guidelines (National Committee for Clinical Laboratory Standards, 2001). A 1–2 × 10^8 colony-forming unit (cfu)/mL inoculum was prepared and adjusted to a final concentration of 1–2 × 10^5 cfu/mL in broth containing samples in two-fold dilutions ranging from 0.0625 µg/mL to 64 µg/mL on a microtiter plate. A culture of *S. aureus* strains in the broth was used as a positive (growth) control, while broth without *S. aureus* was used as a negative control. The minimal inhibitory concentration (MIC) was the lowest concentration that inhibited visible bacterial growth after 24 h of incubation at 35 ± 2°C. Following MIC determination, a time-kill assay was performed using *S. aureus* (ATCC 29213) and a single *S. aureus* (MRSA) strain. A bacterial concentration between 6.1 and 6.5 log cfu/mL was used as the initial inoculum on a microtiter plate. Wells containing Mueller-Hinton broth with mupirocin calcium samples in concentrations of 16 and 8 µg/mL were incubated with *S. aureus* strains for 3, 6 and 24 h at 35 ± 2°C. A minimal bactericidal concentration of 16 µg/mL was previously determined for *S. aureus* (ATCC 29213[20]). After incubation, ten-fold dilutions were prepared with Mueller-Hinton broth and 10-µL samples were subcultured on Mueller-Hinton agar plates. Bacterial colonies were counted after 18 h of incubation at 35 ± 2°C. Experiments were performed in triplicate.

Statistical analysis

Unless otherwise noted, the results are expressed as mean ± standard deviation (SD). A one-way analysis of variance was employed for the comparison of the experimental data. *Post hoc* multiple comparisons were done by Tukey's test for significance at *p*-values less than 0.05 ($p < 0.05$). Mathematical modeling (monoexponential and biexponential equations) was applied to characterize drug release kinetics (GraphPad Prism, GraphPad Software Inc., San Diego, CA; www.graphpad.com). A biexponential model has been used to separate burst (k_1 rate constant) and sustained release phases (k_2 rate constant) of dissolution profiles to enable their comparison[23,24].

Results and discussion

Solvent influence on the properties of the MP

Drug encapsulation, production yield, particle size and morphology

Characteristics of the spray dried MP, differing in DL and solvents used, are given in Table 1. Eudragit® RS solubility in organic solvents was experimentally observed and found to increase in the following order: methanol

Table 1. Characteristics of the MP containing 1:5 and 2:1 (w/w) drug:polymer proportions spray dried from methanol, methanol:ethanol and acetone:isopropanol mixtures.

Samples	Drug:polymer proportion (w/w)	Solvent/s	EE [% ± SD] (n=3)	DL [% ± SD] (n=3)	Yield (%)	RS [% ± SD] (n=3)	PSD [µm ± SD] (n=6) d(0.1)	d(0.5)	D(0.9)
M1	1:5	MeOH	102.3 ± 1.1	16.1 ± 0.2	55.8	0.9 ± 0.0	1.4 ± 0.0	2.8 ± 0.1	7.0 ± 0.2
ME1	1:5	MeOH:EtOH = 50:50(w/w)	99.1 ± 0.9	15.6 ± 0.1	56.0	1.0 ± 0.2	3.4 ± 0.1	7.6 ± 0.2	23.6 ± 0.0
AI1	1:5	Acetone:iPrOH = 40:60(w/w)	99.6 ± 0.6	15.2 ± 0.1	62.6	1.3 ± 0.1	2.6 ± 0.0	5.7 ± 0.0	13.6 ± 0.0
M2	2:1	MeOH	101.5 ± 0.6	63.8 ± 0.3	62.6	1.0 ± 0.1	1.2 ± 0.0	3.1 ± 0.0	10.1 ± 0.2
ME2	2:1	MeOH:EtOH = 50:50(w/w)	99.1 ± 0.8	62.4 ± 0.5	62.7	1.6 ± 0.0	2.0 ± 0.0	3.7 ± 0.0	6.9 ± 0.0
AI2	2:1	Acetone:iPrOH = 40:60(w/w)	99.0 ± 0.6	61.1 ± 0.4	65.8	2.2 ± 0.1	4.1 ± 0.0	9.5 ± 0.0	21.5 ± 0.3

MeOH, methanol; EtOH, ethanol; iPrOH, isopropanol; EE, encapsulation efficacy = percent ratio (w/w %) of the actual drug content in MP and the amount of drug added (theoretical content); DL, drug loading = percent ratio (w/w %) of the drug present in the MP; RD, residual solvents; SD, standard deviation; PSD, particle size distribution.

< methanol:ethanol < acetone:isopropanol. The drug exhibited the opposite order of solubility in regards to the polymer. Irrespective of the solvent used, good encapsulation was achieved for all the MP obtained (EE > 99%; Table 1). There is a high likelihood that the microdroplets formed during atomization will retain their initial composition once they become solid, if they are originally in solution form. These findings are aligned with observations of complete drug encapsulation that was attained by the spray drying process from the feed solution, which were described previously[25–27]. Production yield was generally high for all MP, ranging between 56 and 66% (Table 1).

MP were in the form of white, free-flowing powder (Figure 1). The solvent had a great influence on MP morphology[9,12,28]. Figure 1A–1C represents MP with a drug:polymer proportion of 1:5 (w/w). MP M1 (Figure 1A) were highly shriveled, suggesting that when methanol was used as the solvent, the early onset of the solidification process happened in the drying process, starting with the formation of a pliable layer that later underwent prominent deformation due to the increased interior solvent vapor pressure[9,28]. Methanol:ethanol and acetone:isopropanol mixtures enabled the generation of rather spherical MP, with smooth surfaces and no visible pores (ME1; Figure 1B and AI1; Figure 1C, respectively). Smooth surfaces are often present when a polymer solidifies at a temperature that is high enough to maintain the polymer in the rubbery state (outlet temperatures were between 56 and 69°C), allowing necessary relaxation processes to occur[26]. Ethanol, having a higher boiling point than methanol and being a better solvent for polymer, possibly affected the drying process by slowing down the evaporation rate and delaying solidification. The microdroplet had more time to shrink in size and gradually solidify, thus preserving its spherical shape. An acetone:isopropanol mixture further improved the polymer solubility that again produced sphere-shaped MP without an early surface deposition (and consequential modification of morphology). It is believed that the polymer had a predominant influence on the particle morphology as the DL was at a 15–16% (w/w) level in the associated samples.

Figure 1D–1F represents MP having a drug:polymer proportion of 2:1 (w/w). M2 (Figure 1D) and ME2 (Figure 1E) MP have a regular spherical shape and a smooth and poreless surface. Methanol and methanol:ethanol mixtures allowed the solidification process to happen slowly, resulting in a uniform outward appearance. On the contrary, the acetone:isopropanol mixture significantly reduced the drug solubility while acting as an excellent solvent for the polymer at the same time. Thus, it was expected that the drug would reach its saturation point before the polymer for AI2 MP. These MP (Figure 1F) are not perfectly spherical. Microdroplet coalescence probably happened in close proximity to the atomizer, initiated by extremely rapid drug deposition, thus forming distorted and agglomerated MP.

The PSD results are presented in Table 1. Generally, the small particle sizes (d(0.9) in the range of 7–22 μm) of all MP may be attributed to the relatively low viscosity of the spraying solution (low concentration of solutes) and high compressed nitrogen flow rate. If PSD results are interpreted mutually with SEM images, it is easily recognized that particles are smaller than the measured volume distributions (see d(0.9) values, Table 1). The higher d(0.9) values could be attributed to the agglomerated MP rather than to the actual size of a single particle.

Solid-state characterization

X-ray analyses (Figure 2) have shown composition-dependant halo patterns that are characteristic of highly disordered amorphous forms without diffraction peaks of crystalline mupirocin calcium. However, owing to the low sensitivity of the X-ray technique that was used, there is still a possibility that a very small fraction of crystalline drug is present within the polymer matrix.

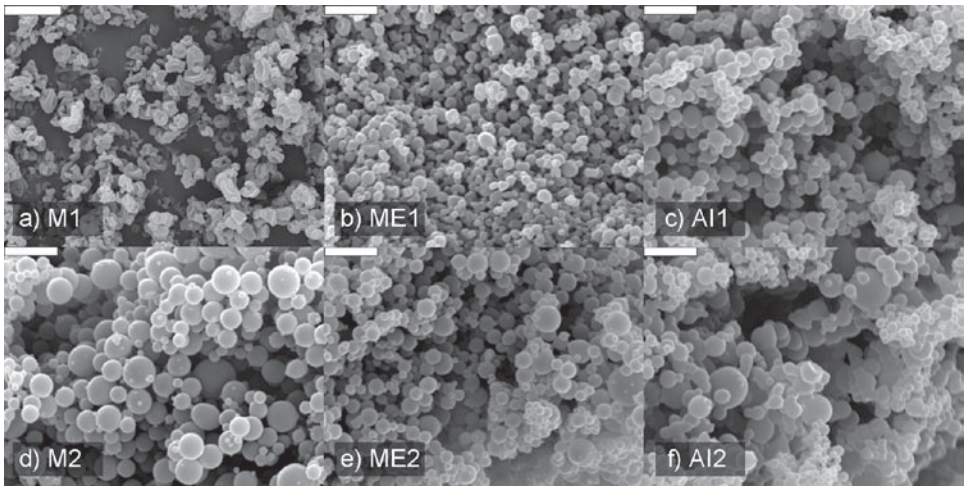

Figure 1. SEM images of the MP: (A) M1, (B) ME1 and (C) AI1 containing 1:5 (w/w) drug:polymer proportions and (D) M2, (E) ME2 and (F) AI2 containing 2:1 (w/w) drug:polymer proportions (size bar denotes 5 μm).

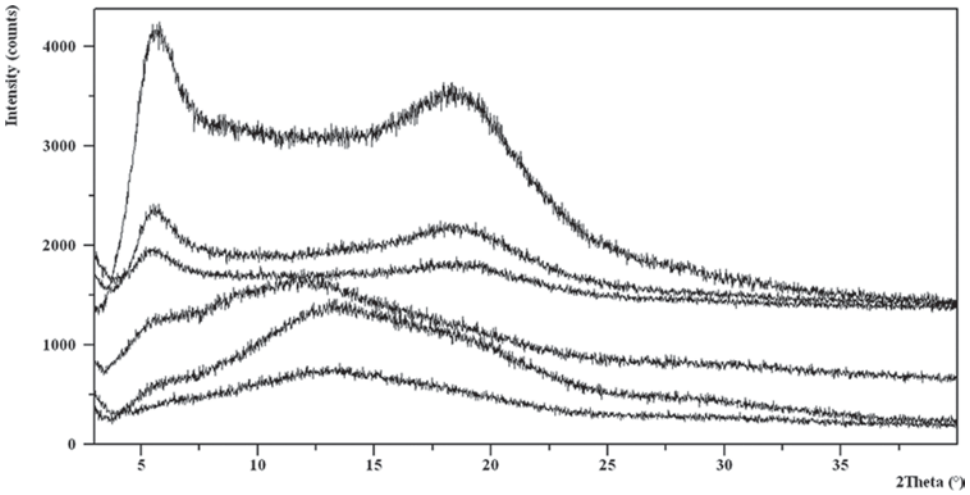

Figure 2. X-ray diffractograms of the MP (from the bottom to the top): (A) M1; (B) ME1; (C) AI1; (D) M2; (E) ME2 and (F) AI2.

Thermal properties are an extremely useful tool in revealing the solid-state form of a drug that is embedded into the polymer matrix, enabling a better understanding of overall MP performance. It also indicates the organization and flexibility of polymer chains that are directly linked to the rate of drug release[29]. The individual thermal properties of the drug and polymer are previously reported in our work[20]. Thermograms of MP containing a 1:5 (w/w) drug:polymer proportion are depicted in Figure 3A. The total heat flow curves generated by MDSC have shown a lack of melting endotherm of mupirocin calcium, which is expected at 133°C (data not shown), assuming an amorphous nature for the obtained systems. These findings were additionally confirmed by the X-ray data (Figure 2). Further, the reverse heat flow curves were utilized to deconvolute the thermal events associated with specific heat that is characteristic for glass transition. A single, primary T_g value has been observed for all MP that indicated the formation of a homogeneous amorphous solid dispersion exhibiting single-phase character[30]. The well-known Gordon-Taylor (GT) equation is nowadays extensively exploited for the prediction of binary mixture behavior based on the free volume theory. It recognizes non-idealities of mixtures in terms of specific drug-polymer interactions or immiscibility issues[31]. Detailed principles underlying this approach are described elsewhere in the literature[31,32] and will not be reported here. However, the calculated GT prediction of the glass transition temperature for a drug:polymer proportion of 1:5 (w/w) was 59.5°C if density differences are neglected. MDSC curves have revealed that different solvents produced solid dispersions of diverse thermal properties that are reflected in altered glass transition temperatures. When methanol was used as a solvent, it yielded MP (M1) with the lowest glass transition temperature (58.4 ± 2.2°C), whereas MP prepared from methanol:ethanol (ME1) and acetone:isopropanol (AI1) mixtures produced solid dispersions with ascending T_g values of 63.4 ± 1.0°C and 68.7 ± 1.1°C, respectively. Such phenomena have already been reported by Al-Obaidi et al[16]. and was attributed to diverse polymer chain conformations caused by different polymer affinities to the solvent. In this particular case, the highest T_g value was observed for the solvent system in which the polymer had the highest solubility. Higher T_g values, positively deviated from the GT prediction, indicate that more energy is required for these mixtures to pass through the glass transition; hence, relatively stronger intermolecular forces could be the cause of the positive deviation observed between measured and predicted T_g values[33]. It should be emphasized also that residual solvents increased from the lowest value for M1 (0.9%, Table 1) to the highest value for AI1 (1.3%, Table 1), so plasticization of the solvent residues could not be related with the observed glass transition temperatures.

FTIR spectra (Figure 4A) of the solid dispersions containing a 1:5 (w/w) drug:polymer proportion were recorded in order to ascertain if any band shift divergence existed amongst the samples. The essentially identical spectra were obtained for the MP and their corresponding physical mixtures, thereby excluding drug-polymer interactions as a root cause of different thermal properties. However, the origin of a T_g increase could be possibly linked to different drug and polymer molecular packing being associated with the decreased free volume as previously reported by Tajber et al[34]. for polyvinylpyrrolidone-based solid dispersions.

Figure 3B represents thermograms of MP having a 2:1 (w/w) drug:polymer proportion. The reverse heat flow curve of M2 and ME2 have shown a single thermal event at 68.1 ± 1.7°C and 66.7 ± 0.6°C, respectively. It confirmed the presence of a drug-polymer solid dispersion with no evidence of phase separation. The calculated GT prediction of the glass transition temperature for a drug:polymer proportion of 2:1 (w/w) was 69.3°C. In this case, GT predicted values corresponded well with experimentally observed glass transition temperatures. However, the reverse heat flow curve for MP prepared from the acetone:isopropanol mixture (AI2) was characterized with two consecutive thermal events appearing at ~61°C and ~68°C, respectively (Figure 3C). Thereby, phase separation being manifested

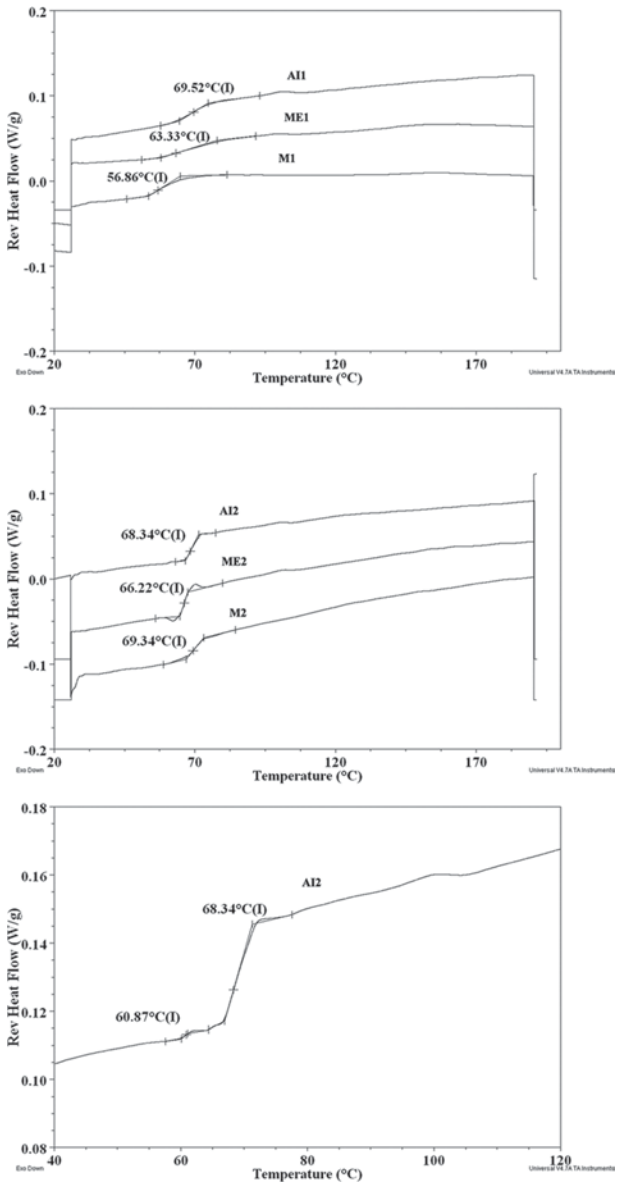

Figure 3. Reverse heat flow curves of the MP: (A) M1, ME1 and AI1 with a 1:5 (w/w) drug:polymer proportion; (B) M2, ME2 and AI2 with a 2:1 (w/w) drug:polymer proportion; (C) zoomed reverse heat flow curve of the AI2 MP.

in two separate glass transition temperatures was verified. Evidently, different solvent systems induced the formation of solid dispersions with different levels of drug mixing with the polymer, under identical compositional and spray drying conditions. Such behavior could be ascribed to poor drug solubility in the particular solvent mixture. Given that drug solubility was tremendously reduced, its high initial saturation could have forced early drug deposition whilst polymer saturation has not yet been achieved in the drying droplet. It is evident that one of the preconditions to achieve simultaneous deposition of drug and polymer is to have similar solubility of both constituents in the common solvents. Janssens et al[35]. just recently demonstrated the importance of drying kinetics to drug-polymer miscibility, as different DLs were achieved when spray drying and film-casting methods were employed. Again, the highest residual solvent level (2.2%, Table 1) was found in the MP prepared from the acetone:isopropanol mixture.

FTIR spectra (Figure 4B) of the solid dispersion containing a 2:1 (w/w) drug:polymer proportion displayed indistinguishable spectral characteristics for the MP and the corresponding physical mixtures, confirming a lack of any interaction.

Drug release behavior

Drug release profiles have shown a high burst release irrespective of the solvent used for the MP having a drug:polymer proportion of 1:5 (w/w) (Figure 5A). High burst release from the MP is extensively reported in the literature[18,36] and presents the major challenge in the development of the controlled release MP. It is described as uncontrolled drug release, which occurs immediately after MP come into contact with dissolution medium[18], and is frequently attributed to the surface-associated or heterogeneously-distributed drug within the particle. It may also be caused by high porosity or low density of MP[36]. Moreover, the small length scale associated with MP supports rapid release unless it is suppressed by a slow diffusion coefficient and low drug solubility[2].

Drug release from MP was compared with crystalline and amorphous drug release patterns. Mono- and biexponential mathematical models were applied to characterize drug release patterns, and their fits were compared using an extra sum-of-squares F-test (Table 2). As the best fit was attained using a biexponential model, existence of a distinct burst and sustained phases of drug release were proven for all MP. The burst release of samples containing a 1:5 (w/w) drug:polymer proportion ranged between 62.8 ± 3.6% and 69.7 ± 2.0% (A parameter, Table 2) with rate constants ranging between 0.336 ± 0.024 and 0.457 ± 0.073 min^{-1}, showing no significant difference among them ($p > 0.05$).

One of the causes of the rapid initial burst release could be the change in the physical form of the drug, from the crystalline into the amorphous, which promoted its solubility. But, it is evident that MP achieved a slower drug release when compared with the amorphous drug (Figure 5A). Particle size difference had no major impact on drug release behavior of the MP having a drug:polymer proportion of 1:5 (w/w). Drug release profiles were not affected by the particle size even if MP M1 and ME1 are compared for which the most prominent size difference was observed. As previously reported by our group, fast drug release might have been supported by a rapid polymer deposition linked to high initial saturation. By varying feed solvents, we intended to increase polymer solubility and delay its solidification. This variation, however, resulted in modified physical properties but has not provided significant improvement in prolonging drug release. Even though the glass transition temperature was higher for the MP prepared from the acetone:isopropanol mixture, presuming denser matrices (as no stronger drug-polymer interaction was proven), it has not provided a slower drug release. It is possible that the decrease of

drug solubility in a solvent that promoted polymer solubility was an obstacle to achieving better release control. Lower drug solubility could have induced earlier deposition, resulting in surface drug-enriched regions. It is eventually important to inhibit fast deposition of either component if a prolonged release pattern is desired.

The MP having a 2:1 (w/w) drug:polymer proportion gave different dissolution patterns as shown in

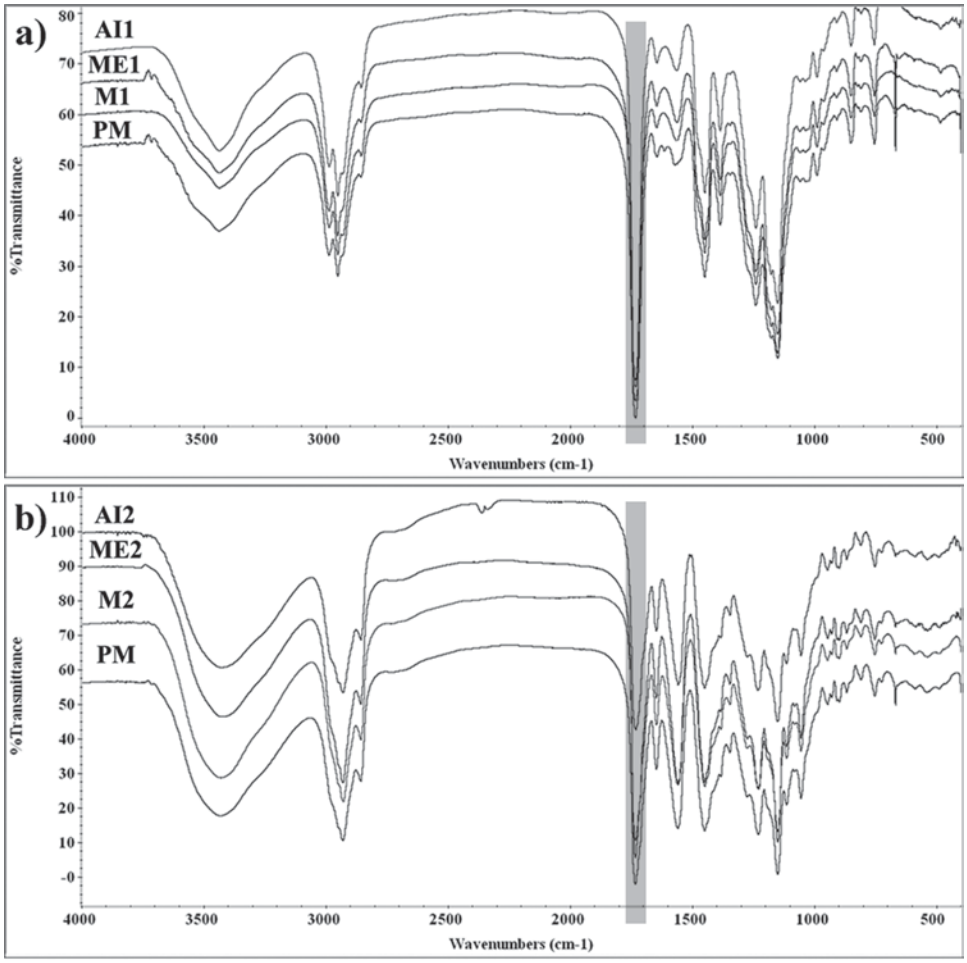

Figure 4. FTIR spectra of the MP: (A) M1, ME1, AI1 and physical mixtures (PM) with a 1:5 (w/w) drug:polymer proportion and (B) M2, ME2, AI2 and physical mixtures (PM) with a 2:1 (w/w) drug:polymer proportion.

Table 2. Mathematical modelling parameters of mupirocin calcium release from the MP containing 1:5 and 2:1 (w/w) drug:polymer proportions spray dried from methanol, methanol:ethanol and acetone:isopropanol mixtures (initially and after storage for 10 months at 25°C/60%RH).

	Monoexponential model $Q = a(1 - e^{-kt})$			Biexponential model $Q = A(1 - e^{-k_1 t}) + B(1 - e^{-k_2 t})$				
Sample	R^2	a (% ± SEM)	k (min^{-1} ± SEM)	R^2	A (% ± SEM)	k_1 (min^{-1} ± SEM)	B (% ± SEM)	k_2 (min^{-1} ± SEM)
M1	0.980	78.3 ± 1.0	0.270 ± 0.024	0.996 (0.994)	62.8 ± 3.6 (50.3 ± 5.2)	0.457 ± 0.073 (0.550 ± 0.038)	19.5 ± 4.9 (23.4 ± 6.6)	0.033 ± 0.008 (0.038 ± 0.010)
ME1	0.982	83.8 ± 1.0	0.286 ± 0.025	0.998 (0.996)	69.7 ± 2.0 (57.6 ± 7.0)	0.455 ± 0.044 (0.640 ± 0.051)	19.0 ± 3.0 (25.8 ± 8.1)	0.027 ± 0.005 (0.051 ± 0.012)
AI1	0.990	85.1 ± 0.8	0.220 ± 0.013	0.999 (0.974)	67.3 ± 3.4 (54.7 ± 11.2)	0.336 ± 0.024 (0.422 ± 0.033)	20.7 ± 4.0 (37.6 ± 14.7)	0.042 ± 0.007 (0.033 ± 0.013)
M2	0.954	82.7 ± 2.4	0.047 ± 0.006	0.991 (0.991)	31.8 ± 5.3 (44.4 ± 6.5)	0.348 ± 0.113 (0.423 ± 0.036)	55.8 ± 7.7 (34.8 ± 8.3)	0.024 ± 0.003 (0.036 ± 0.008)
ME2	0.941	75.6 ± 2.2	0.062 ± 0.009	0.993 (0.997)	37.2 ± 3.9 (39.5 ± 3.3)	0.336 ± 0.076 (0.552 ± 0.033)	45.3 ± 6.1 (44.6 ± 4.6)	0.022 ± 0.003 (0.030 ± 0.003)
AI2	0.953	85.1 ± 1.8	0.119 ± 0.016	0.986 (0.996)	45.5 ± 9.9 (76.6 ± 1.8)	0.434 ± 0.193 (0.505 ± 0.005)	44.9 ± 12.3 (24.3 ± 18.1)	0.037 ± 0.009 (0.030 ± 0.006)

Q, percentage of drug released at time t; k, k_1 and k_2, rate constants; a, plateau value; A and B, the parameters which reflect the portion of the released drug that contributed to the burst and sustained phases, respectively; R^2, coefficient of determination; SEM, standard error; non-bracketed and bracketed values denote initial and 10-month stability data, respectively.

Figure 5B. Mathematical modeling confirmed that a biexponential model was more suitable for drug release as compared to a monoexponential model (Table 2). MP prepared from the methanol (M2) and methanol:ethanol mixture (ME2) displayed almost identical release patterns, with the burst releases ranging between 31.8 ± 5.3% and 37.2 ± 3.9% (A parameter, Table 2), respectively. MP prepared from the acetone:isopropanol mixture (AI2) were characterized with a higher initial release (45.5 ± 9.9%, Table 2) and a burst constant rate of 0.434 ± 0.193 min^{-1}. Again, PSDs of MP having 2:1 (w/w) drug:polymer proportion cannot explain differences observed in drug release profiles. Smaller M2 and ME2 MP obtained slower drug release in comparison to the bigger and more agglomerated AI2 MP. It is assumed that due to altered drug-polymer miscibility in AI2 MP, certain amount of the drug was separated from the polymer matrix and was thus readily available for the dissolution process. This assumption could be supported by the thermal properties of the corresponding MP, for which phase separation was determined (Figure 3C). In addition, drug solubility in the acetone:isopropanol mixture was low, and its deposition started earlier in the drying process, which stopped shrinkage of the microdroplets and precluded generation of a coherent matrix. Comparing the release profiles of M2 and ME2 MP with mupirocin calcium dissolution profiles, it is noticeable that MP provided remarkable control over drug release. Specifically, if the amorphous drug and above-mentioned MP (that contain amorphous drug within polymer matrix) are mutually considered, a substantially decreased drug release was accomplished.

Physical stability of the MP

Solid-state characterization

X-ray diffractograms of the MP upon storage for 10 months at 25°C/60%RH are provided in Figure 6. Clearly, crystallization cannot be observed and solid dispersions generated in the spray drying process remained amorphous during storage regardless of the drug:polymer proportion or the solvent used. However, it is not only the crystallization of drug that could deteriorate MP performance, but also any change in molecular structure including the distribution of the drug within the polymer.

Reverse heat flow curves of the MP with lower DL (1:5 (w/w) drug:polymer proportion) are given in

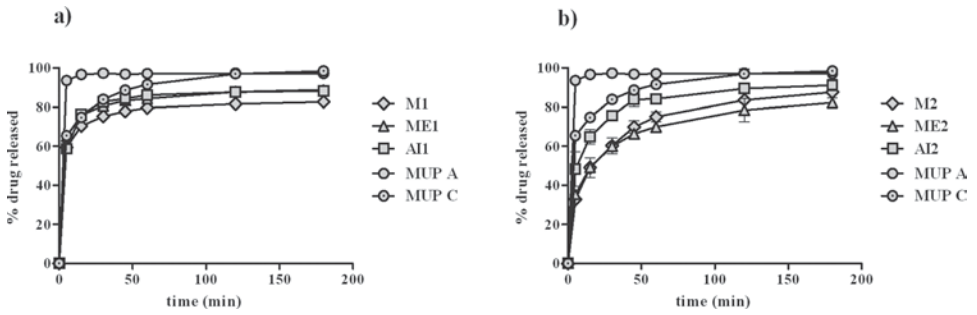

Figure 5. *In vitro* drug release profiles of the MP (A) M1, ME1 and AI1 with a 1:5 (w/w) drug:polymer proportion and (B) M2, ME2 and AI2 with a 2:1 (w/w) drug:polymer proportion in comparison to the drug (amorphous (A) and crystalline (C)). Data are the mean ± SD ($n = 3$). In some cases, the error bars are within the size of the data point.

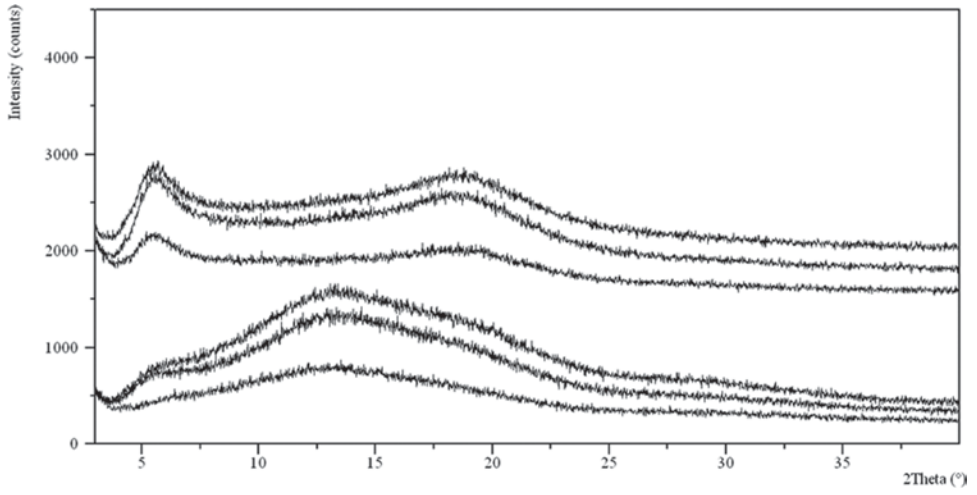

Figure 6. X-ray diffractograms of the MP after storage for 10 months at 25°C/60%RH (from the bottom to the top): (A) M1; (B) ME1; (C) AI1; (D) M2; (E) ME2 and (F) AI2.

Figure 7A. All thermograms were characterized by a single glass transition event, but shifted slightly toward higher temperatures in comparison to the T_gs obtained at the beginning of the stability study. The glass transition temperatures for the M1, ME1 and AI1 MP were 61.0 ± 0.6°C, 66.4 ± 0.5°C and 72.2 ± 1.0°C, respectively. There was no evidence of a thermal event associated with the melting of the crystalline drug. Storage of the amorphous MP did not trigger crystallization processes but certain changes of the thermal properties were manifested. As a result of rapid solvent removal during the spray drying process, polymer chains are immobilized while trying to reach equilibrium[18,37]. The increase of T_g detected during storage may be attributed to local molecular rearrangement of polymeric chains in any free space available, as the polymer progresses toward thermal equilibrium.

Reverse heat flow curves of the MP with a 2:1 (w/w) drug:polymer proportion (Figure 7B and 7C) revealed that M2 and ME2 MP remained unchanged with T_g values of 67.7 ± 2.2°C and 67.2 ± 1.3°C, respectively. Even though they are amorphous in nature, these systems retained their initial structure. Sometimes, the drug that was incorporated into the polymer matrix acts like an antiplasticizer, slowing down the physical aging of the matrix and hindering the relaxation processes of amorphous material[17]. Thermograms obtained for the AI2 MP (Figure 7C) differed from the other MP as two distinct thermal events were observed. The phase separation seen at the beginning of the stability study was even more pronounced after storage, showing the first thermal event at ~66°C and the second at ~74°C.

Drug release behavior

Almost the same dissolution behavior was obtained for the MP containing a 1:5 (w/w) drug:polymer proportion after storage for 10 months. Mathematical modeling has proven that all dissolution profiles matched biexponential equations (Table 2). The burst releases for these MP ranged between 50.3 ± 5.2 and 57.6 ± 7.0% (A parameter, Table 2), while the burst rate constants varied between 0.422 ± 0.033 and 0.640 ± 0.051 min^{-1}. Statistical analyses confirmed that burst releases as well as rate constants have not changed significantly during storage ($p > 0.05$). Regarding MP containing a 2:1 (w/w) drug:polymer proportion, the burst releases of 44.4 ± 6.5 and 39.5 ± 3.3% and rate constants of 0.423 ± 0.036 and 0.552 ± 0.033 min^{-1} that were calculated for the M2 and ME2 MP, respectively, did not differ significantly from the initially obtained values. However, AI2 MP were characterized by an exceptionally high initial release (76.6 ± 1.8%, Table 2) with a burst release rate constant of 0.505 ± 0.005 min^{-1}. A significant change in the dissolution profile is apparent for AI2 MP, proving that the physical aging of samples seriously ruined initial MP characteristics.

Conclusively, samples have not undergone substantial crystallization during storage. This could be attributed to the low crystallization propensity of the mupirocin calcium as well as the ability of the polymer matrix to provide an energy barrier for such a process. The minor shifts of glass transition temperatures for a 1:5 (w/w) drug:polymer proportion substantiated the aging processes but have not influenced drug release patterns. Nonetheless, the MP with a 2:1 (w/w) drug:polymer proportion, prepared from methanol and a methanol:ethanol mixture, remained physically stable and maintained the original release profile. At the same time, a prominent phase separation was confirmed for the AI2 MP, which contributed to the considerable burst release.

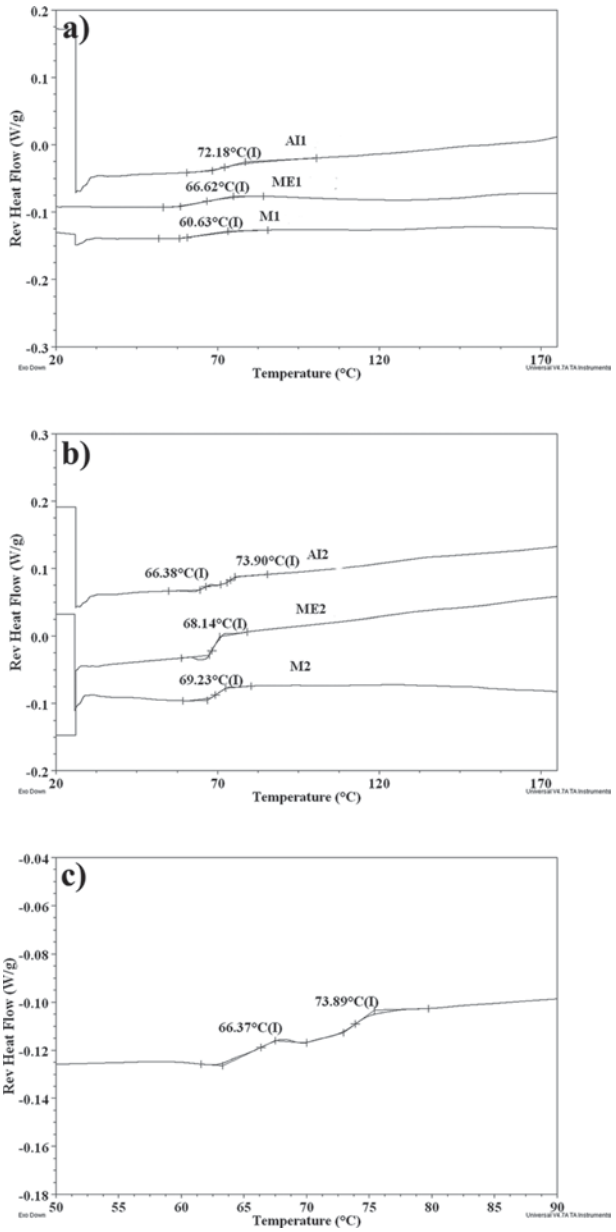

Figure 7. Reverse heat flow curves of the MP after storage for 10 months at 25°C/60%RH: (A) M1, ME1 and AI1 with a 1:5 (w/w) drug:polymer proportion; (B) M2, ME2 and AI2 with a 2:1 (w/w) drug:polymer proportion; (C) zoomed reverse heat flow curve of the AI2 MP.

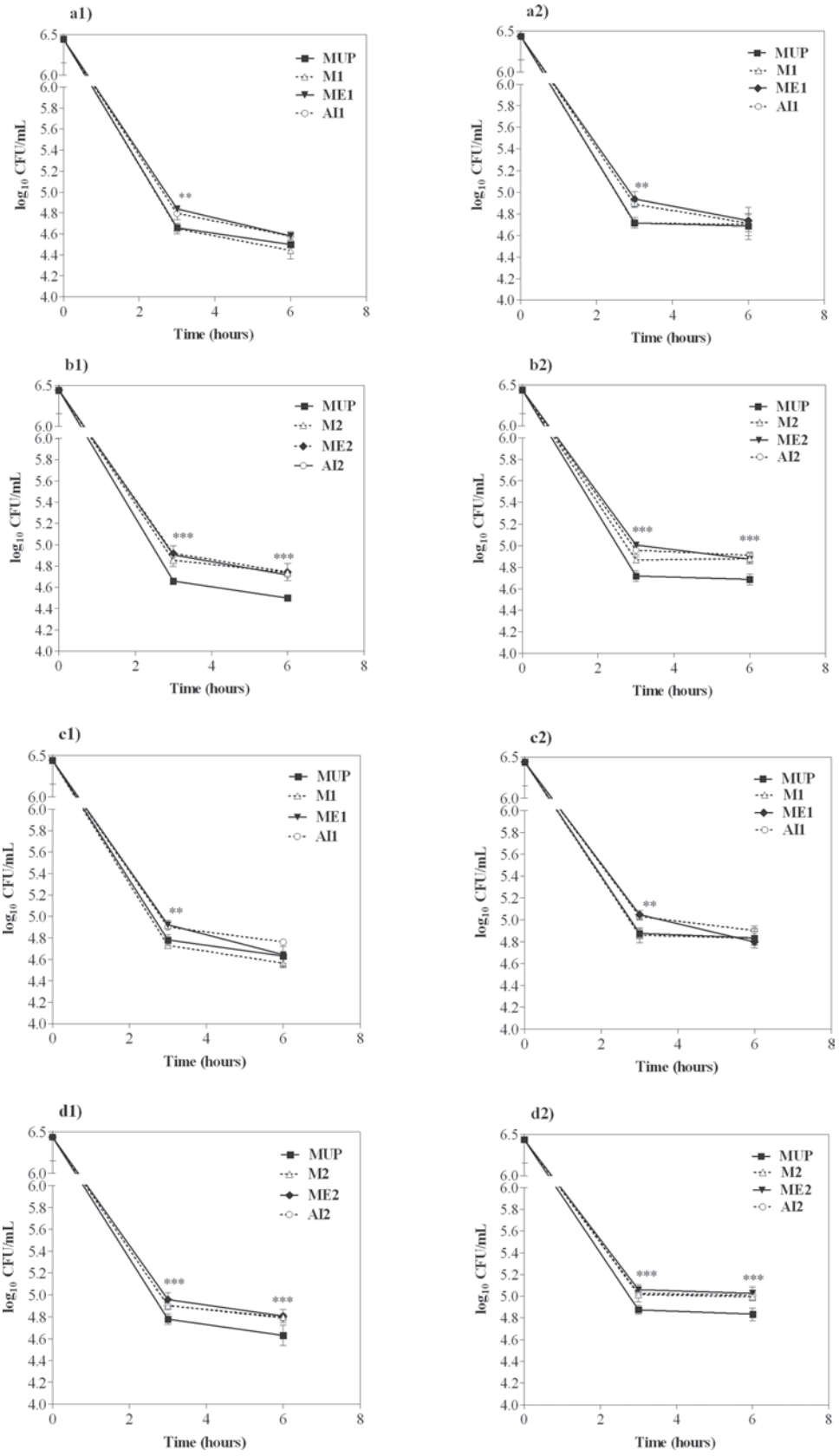

Figure 8. Time-kill curves for *S. aureus* ATCC 29213 (A1–D1) and *S. aureus* MRSA strains (A2–D2) exposed to free drug and MP at concentrations of 16 μg/mL (A,B) and 8 μg/mL (C,D) for 3 and 6 h. The asterisk represents a significant difference ($p < 0.05$) between MP and the free drug.

Antimicrobial activity of the MP

Time-kill assay curves for the MP are appraised, along with the drug, as presented in Figure 8. The MIC for *S. aureus* (ATCC 29213) was 0.125 μg/mL for all tested samples after 24 h of incubation, which was in agreement with our previous results. MIC values for *S. aureus* (MRSA) strains were between 0.25 and 0.5 μg/mL, which were found susceptible according to the published recommendation[38]. After 3 h of incubation, drug and M1 applied at concentrations of 16 and 8 μg/mL demonstrated a similar drop in colony counts of both tested *S. aureus* strains (4.6–4.7 and 4.7–4.9 log cfu/mL, respectively). Samples ME1 and AI1 were significantly different from the free drug, producing a drop to 4.8–4.9 and 4.8–5.0 log cfu/mL for ATCC 29213 and MRSA, respectively. However, upon 6 h of incubation, no significant difference was observed between the antimicrobial activity of MP and the free drug at both tested concentrations, which might be attributed to the complete drug release from the tested microsystems.

MP having a 2:1 (w/w) drug:polymer proportion (M2, ME2, AI2) were significantly less effective in comparison with the free drug ($p < 0.05$), both after 3 and 6 h of incubation (Figure 8). These results of antimicrobial activity validate the drug release data, proving that the desired prolonged release was attained even with superior DL. All tested samples showed similar antimicrobial activity after 24 h (data not presented). Colony counts of *S. aureus* (ATCC 29213) that were exposed to 16 μg/mL for 24 h dropped to approximately 3.9 log cfu/mL, which corresponds to a 99.7% reduction of initial inoculum, while a concentration of 8 μg/mL decreased the bacterial concentration to approximately 4.2 log cfu/mL (99.3% reduction). MRSA counts dropped to 4.3 log cfu/mL (99.3% reduction) and 4.5 cfu/mL (99% reduction), respectively. These findings substantiate that the incorporation of drug into the polymer did not compromise its antibacterial activity. Despite the high bactericidal concentrations employed, the time-kill assay was sensitive enough to detect differences between the drug and MP, providing strong evidence of the ability of the MP to prolong drug release. It is also important to note that any prospective usage of such microsystems in skin therapy requires adjustment of the initial dose of a once-a-day formulation.

Conclusions

Evaluation of spray dried Eudragit® RS-based mupirocin calcium-loaded MP provided evidence that the feed solvent influenced the physical characteristics, stability and performance of MP. Drug-polymer miscibility and the corresponding thermal properties, morphology, drug release and antimicrobial activity were dependent on the DL and the solvent used. The superior control of drug release from MP was achieved with a higher DL (2:1 (w/w) drug:polymer proportion) using solvents in the following order: methanol ≈ methanol:ethanol (50:50) > isopropanol:acetone (40:60). The influence of the solvent on the morphology was less pronounced for particular DL, but it altered drug-polymer miscibility, conceivably as a result of different solidification kinetics. Moreover, a time-kill assay performed on *S. aureus* (ATCC 29213) and methicillin-resistant *S. aureus* (MRSA) confirmed a prolonged release and preservation of antimicrobial activity of encapsulated drug. Irrespective of the solvents used, the lower DL (1:5 (w/w) drug:polymer proportion) yielded less control over the drug, as supported by the drug release and antimicrobial activity data. For this drug:proportion, the solvent affected the thermal properties, but without a noteworthy impact on performance. Generally, good stability upon storage was obtained, excluding MP with a phase separation that was present initially.

Declaration of interest

The authors report no conflicts of interest.

References

1. Re MI. (2006). Formulating drug delivery systems by spray drying. Drying Technology, 24:433–446.
2. Vehring R. (2008). Pharmaceutical particle engineering via spray drying. Pharm Res, 25:999–1022.
3. Soundrapandian C, Basu D, Sa B, Datta S. (2011). Local drug delivery system for the treatment of osteomyelitis: *In vitro* evaluation. Drug Dev Ind Pharm, 37:538–546.
4. Jain D, Carvalho E, Banthia AK, Banerjee R. (2011). Development of polyvinyl alcohol-gelatin membranes for antibiotic delivery in the eye. Drug Dev Ind Pharm, 37:167–177.
5. Freiberg S, Zhu XX. (2004). Polymer microspheres for controlled drug release. Int J Pharm, 282:1–18.
6. Hadinoto K, Cheow WS. (2009). Hollow spherical nanoparticulate aggregates as potential ultrasound contrast agent: Shell thickness characterization. Drug Dev Ind Pharm, 35:1167–1179.
7. Nekkanti V, Muniyappan T, Karatgi P, Hari MS, Marella S, Pillai R. (2009). Spray-drying process optimization for manufacture of drug-cyclodextrin complex powder using design of experiments. Drug Dev Ind Pharm, 35:1219–1229.
8. Miller-Chou BA, Koenig JL. (2003). A review of polymer dissolution. Prog Polym Sci, 28:1223–1270.
9. Raula J, Eerikäinen H, Kauppinen EI. (2004). Influence of the solvent composition on the aerosol synthesis of pharmaceutical polymer nanoparticles. Int J Pharm, 284:13–21.
10. Wulsten E, Kiekens F, van Dycke F, Voorspoels J, Lee G. (2009). Levitated single-droplet drying: Case study with itraconazole dried in binary organic solvent mixtures. Int J Pharm, 378:116–121.
11. Esposito E, Roncarati R, Cortesi R, Cervellati F, Nastruzzi C. (2000). Production of Eudragit microparticles by spray-drying technique: Influence of experimental parameters on morphological and dimensional characteristics. Pharm Dev Technol, 5:267–278.
12. Gander B, Wehrli E, Alder R, Merkle HP. (1995). Quality improvement of spray-dried, protein-loaded D,L-PLA microspheres by appropriate polymer solvent selection. J Microencapsul, 12:83–97.
13. Zhang ZY, Ping QN, Xiao B. (2000). Microencapsulation and characterization of tramadol-resin complexes. J Control Release, 66:107–113.
14. Bain DF, Munday DL, Smith A. (1999). Solvent influence on spray-dried biodegradable microspheres. J Microencapsul, 16:453–474.

15. Luna-Barcenas G, Meredith JC, Sanchez IC, Johnston KP. (1997). Relationship between polymer chain conformation and phase boundaries in a supercritical fluid. J Chem Phys, 107:10782–10792.
16. Al-Obaidi H, Brocchini S, Buckton G. (2009). Anomalous properties of spray dried solid dispersions. J Pharm Sci, 98:4724–4737.
17. Rosilio V, Deyme M, Benoit JP, Madelmont G. (1998). Physical aging of progesterone-loaded poly(D,L,-lactide-co-glycolide) microspheres. Pharm Res, 15:794–798.
18. Allison SD. (2008). Effect of structural relaxation on the preparation and drug release behavior of poly(lactic-co-glycolic)acid microparticle drug delivery systems. J Pharm Sci, 97:2022–2035.
19. Sipos P, Szabó A, Erős I, Szabó-Révész P. (2008). A DSC and Raman spectroscopic study of microspheres prepared with polar cosolvents by different techniques. J Therm Anal Calorim, 94:109–118.
20. Dürrigl M, Kwokal A, Hafner A, Segvic Klaric M, Dumicic A, Cetina-Cižmek B et al. (2011). Spray dried microparticles for controlled delivery of mupirocin calcium: Process-tailored modulation of drug release. J Microencapsul, 28:108–121.
21. Parenti MA, Hatfield SM, Leyden JJ. (1987). Mupirocin: A topical antibiotic with a unique structure and mechanism of action. Clin Pharm, 6:761–770.
22. Embil K, Nacht S. (1996). The Microsponge Delivery System (MDS): A topical delivery system with reduced irritancy incorporating multiple triggering mechanisms for the release of actives. J Microencapsul, 13:575–588.
23. Beck RC, Pohlmann AR, Hoffmeister C, Gallas MR, Collnot E, Schaefer UF et al. (2007). Dexamethasone-loaded nanoparticle-coated microparticles: Correlation between *in vitro* drug release and drug transport across Caco-2 cell monolayers. Eur J Pharm Biopharm, 67:18–30.
24. Lionzo MI, Ré MI, Guterres SS, Pohlmann AR. (2007). Microparticles prepared with poly(hydroxybutyrate-co-hydroxyvalerate) and poly(epsilon-caprolactone) blends to control the release of a drug model. J Microencapsul, 24:175–186.
25. Rassu G, Gavini E, Spada G, Giunchedi P, Marceddu S. (2008). Ketoprofen spray-dried microspheres based on Eudragit RS and RL: Study of the manufacturing parameters. Drug Dev Ind Pharm, 34:1178–1187.
26. Wang FJ, Wang CH. (2002). Effects of fabrication conditions on the characteristics of etanidazole spray-dried microspheres. J Microencapsul, 19:495–510.
27. Palmieri GF, Bonacucina G, Di Martino P, Martelli S. (2001). Spray-drying as a method for microparticulate controlled release systems preparation: Advantages and limits. I. Water-soluble drugs. Drug Dev Ind Pharm, 27:195–204.
28. Rizi K, Green RJ, Donaldson M, Williams AC. (2011). Production of pH-responsive microparticles by spray drying: Investigation of experimental parameter effects on morphological and release properties. J Pharm Sci, 100:566–579.
29. da Silva AA Jr, de Matos JR, Formariz TP, Rossanezi G, Scarpa MV, do Egito ES et al. (2009). Thermal behavior and stability of biodegradable spray-dried microparticles containing triamcinolone. Int J Pharm, 368:45–55.
30. DiNunzio JC, Hughey JR, Brough C, Miller DA, Williams RO 3rd, McGinity JW. (2010). Production of advanced solid dispersions for enhanced bioavailability of itraconazole using KinetiSol Dispersing. Drug Dev Ind Pharm, 36:1064–1078.
31. Hancock BC, Zografi G. (1997). Characteristics and significance of the amorphous state in pharmaceutical systems. J Pharm Sci, 86:1–12.
32. Weuts I, Kempen D, Decorte A, Verreck G, Peeters J, Brewster M et al. (2004). Phase behaviour analysis of solid dispersions of loperamide and two structurally related compounds with the polymers PVP-K30 and PVP-VA64. Eur J Pharm Sci, 22:375–385.
33. van Drooge DJ, Hinrichs WL, Visser MR, Frijlink HW. (2006). Characterization of the molecular distribution of drugs in glassy solid dispersions at the nano-meter scale, using differential scanning calorimetry and gravimetric water vapour sorption techniques. Int J Pharm, 310:220–229.
34. Tajber L, Corrigan OI, Healy AM. (2005). Physicochemical evaluation of PVP-thiazide diuretic interactions in co-spray-dried composites–analysis of glass transition composition relationships. Eur J Pharm Sci, 24:553–563.
35. Janssens S, De Zeure A, Paudel A, Van Humbeeck J, Rombaut P, Van den Mooter G. (2010). Influence of preparation methods on solid state supersaturation of amorphous solid dispersions: A case study with itraconazole and Eudragit e100. Pharm Res, 27:775–785.
36. Yeo Y, Park K. (2004). Control of encapsulation efficiency and initial burst in polymeric microparticle systems. Arch Pharm Res, 27:1–12.
37. Bouissou C, Rouse JJ, Price R, van der Walle CF. (2006). The influence of surfactant on PLGA microsphere glass transition and water sorption: Remodeling the surface morphology to attenuate the burst release. Pharm Res, 23:1295–1305.
38. Kresken M, Hafner D, Schmitz FJ, Wichelhaus TA; Paul-Ehrlich-Society for Chemotherapy. (2004). Prevalence of mupirocin resistance in clinical isolates of *Staphylococcus aureus* and *Staphylococcus epidermidis*: Results of the Antimicrobial Resistance Surveillance Study of the Paul-Ehrlich-Society for Chemotherapy, 2001. Int J Antimicrob Agents, 23:577–581.